

Supporting Information

Wide Visible-Range Activatable Fluorescence ZnSe:Eu³⁺/Mn²⁺@ZnS Quantum Dots: Local Atomic Structure Order and Application as a Nanoprobe for Bioimaging

Zahid U. Khan^{*a,b}, Mayara K. Uchiyama^b, Latif U. Khan^{*b,c}, Hiro Goto^d, Koiti Araki^b, Maria C. F. C. Felinto^e, Ana O. De Souza^f, Hermi F. Brito^{*b}, Magnus Gidlund^a

^aDepartment of Immunology, Institute of Biomedical Sciences-IV, University of São Paulo (USP), Zip Code 05508-000, São Paulo-SP, Brazil.

^bDepartment of Fundamental Chemistry, Institute of Chemistry, University of São Paulo (USP), Zip Code 05508-000, São Paulo-SP, Brazil.

^cSynchrotron-light for Experimental Science and Applications in the Middle East (SESAME) P.O. Box 7, Allan 19252, Jordan.

^dFaculdade de Medicina, Universidade de São Paulo (USP), Zip Code 05403-000, São Paulo-SP, Brazil.

^eInstitute of Nuclear Energy and Research, Zip Code 05508-000, University of São Paulo (USP), São Paulo-SP, Brazil.

^fDevelopment and Innovation Laboratory, Butantan Institute, Zip Code 05503-900, São Paulo-SP, Brazil.

Corresponding Emails: latifullah.khan@sesame.org.jo (Latif U. Khan); hefbrito@iq.usp.br (Hermi F. Brito)

1. Water conversion (ligand exchange)

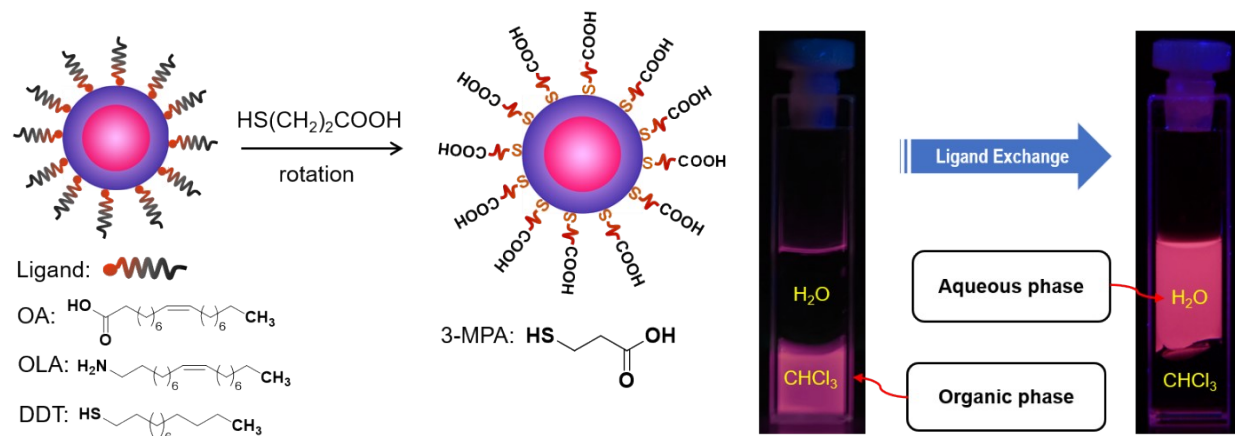


Figure S1. Schematic representation and digital photographs of phase transfer of ZnS passivated ZnSe:xEu³⁺,yMn²⁺ (x, y = 12 mol%) core/shell QDs solution from chloroform layer to water layer after ligand exchange reaction, under UV irradiation hand lamp ($\lambda = 365$ nm).

2. FTIR spectroscopy analyses

The FTIR spectra of DDT/OA/OLA capped ZnSe: $x\text{Eu}^{3+}$, $y\text{Mn}^{2+}$ @ZnS QDs exhibited characteristic absorption bands centered at 2955 cm^{-1} (asymmetric vibration of CH_3), 2922 cm^{-1} (asymmetric stretching of CH_2), 2855 cm^{-1} (symmetric stretching of CH_2), 1554 cm^{-1} and 1436 cm^{-1} (asymmetric and symmetric vibration of COO), 1460 cm^{-1} (scissoring mode of CH_2), and 722 cm^{-1} (rocking band of CH_2). After ligand exchange reaction, the peaks shifted to new positions corresponding to 3-MPA capping agent. The pronounced peaks positions centered at 3396 cm^{-1} (νOH), 1558 cm^{-1} (νCOO^-), 1402 cm^{-1} (νCOO^-), and 1045 cm^{-1} (δOH) indicate the successful functionalization of QDs with 3-MPA. The carboxylate anions can be resulted from the deprotonation by reacting with NaOH base.

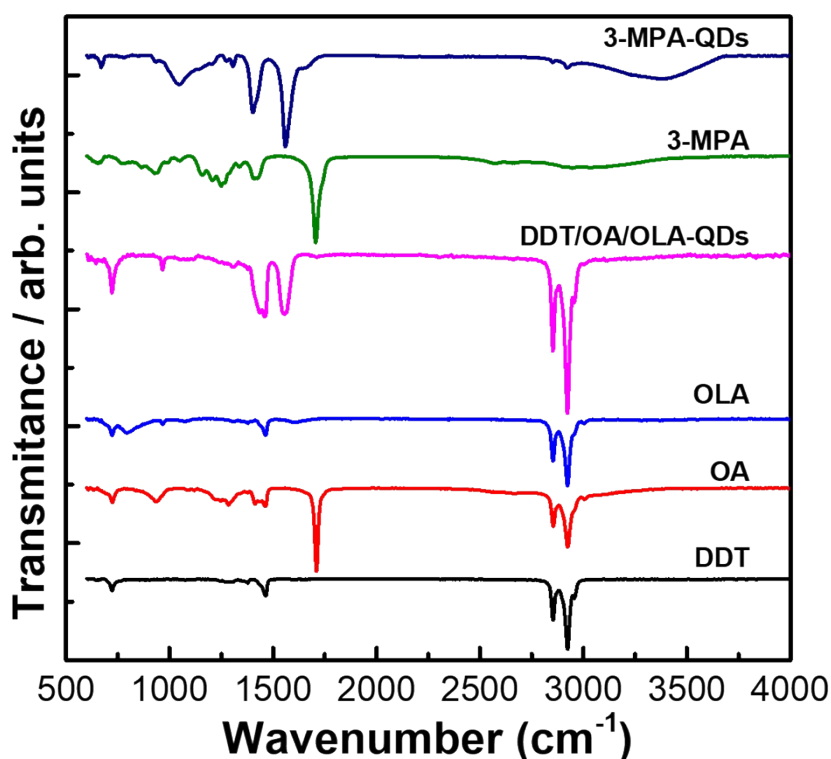


Figure S2. FTIR spectra of the 1-dodecanthiol (DDT), oleic acid (OA), oleylamine (OLA) and 3-mercaptopropionic acid (3-MPA) ligands and ZnSe: $x\text{Eu}^{3+}$, $y\text{Mn}^{2+}$ @ZnS core/shell QDs before and after ligand exchange reaction (DDT/OA/OLA-capped QDs and 3-MPA-capped QDs).

3. X-ray diffraction patterns

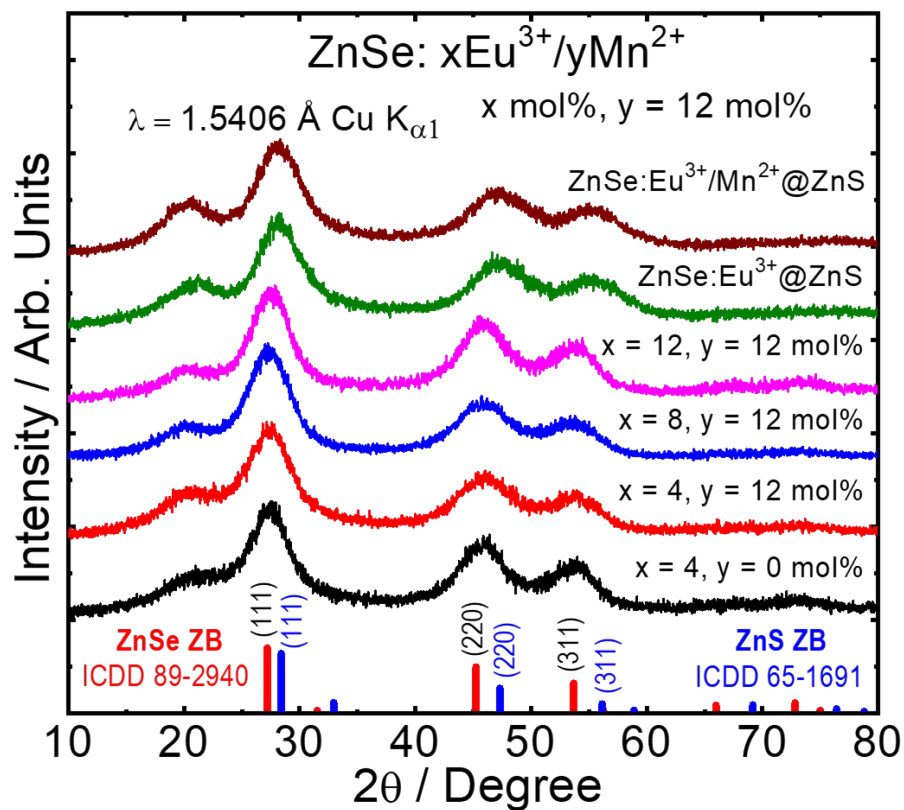


Figure S3. X-ray powder diffraction patterns of ZnSe:xEu³⁺,yMn²⁺ (x = 4, 8, and 12; y = 12 mol%) nanocrystals and 4 MLs of ZnS passivated ZnSe:xEu³⁺,yMn²⁺ (x, y = 12 mol%) and ZnSe:Eu³⁺ (4 mol%) core/shell QDs.

4. Hydrodynamic size and zeta potential

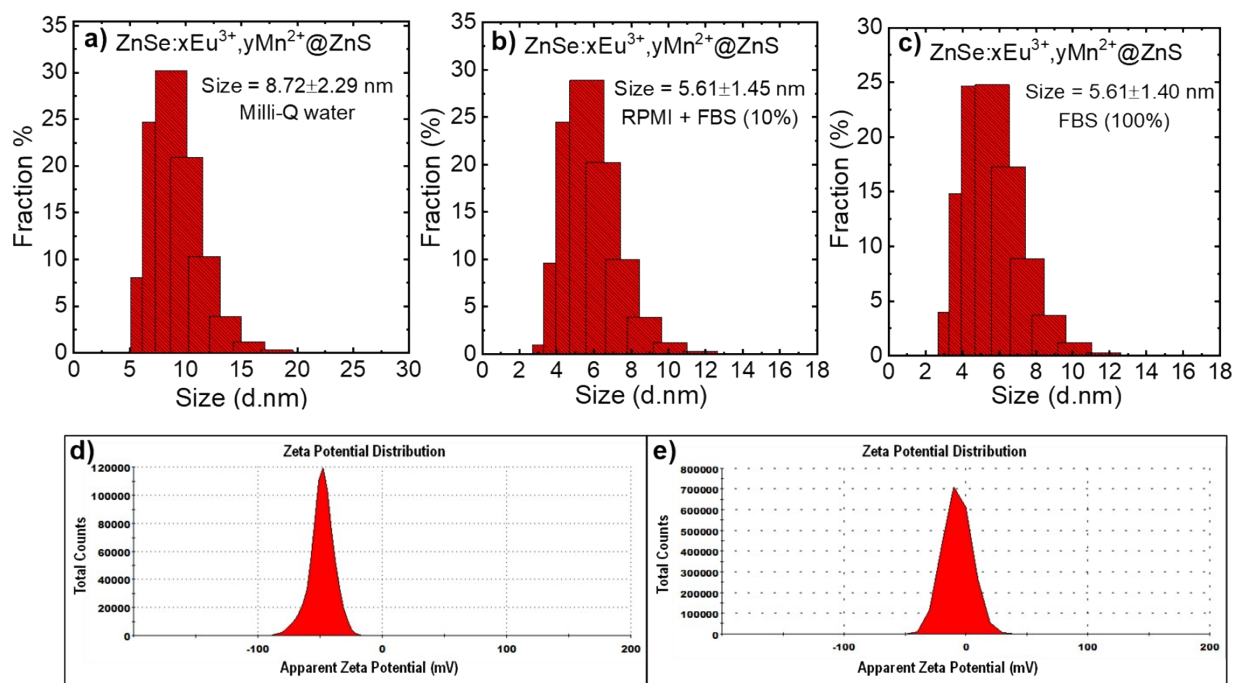


Figure S4. Size-distribution histogram of ZnSe:xEu³⁺,yMn²⁺@ZnS (x, y = 12 mol%) core/shell QDs in different solvent systems, Milli-Q water (a), RPMI supplemented with FBS (10%) (b) and pure FBS (100%) (c). Zeta potential of QDs in different media, Milli-Q water (d) and RPMI supplemented with FBS (10%) (e).

5. XAFS data measurement and analysis

The X-ray absorption fine structure (XAFS) measurements were performed on the XAFS/XRF beamline, Synchrotron-Light for Experimental Science and Applications in the Middle East (SESAME), operating at 2.5 GeV in “decay” mode with a maximum electron current of 250 mA. The Zn K-edge (9659 eV) XAFS spectra of all the QDs were measured in transmission mode at room temperature, monitoring X-ray beam intensity before and after the sample by two ionization chambers filled with a mixture of noble gases. Whereas, XAFS spectra of the Eu and Mn dopants were acquired in fluorescence mode with a Silicon Drift Detectors (SDD), KETEK GmbH, in their respective spectral range of Eu L₃-edge (6977 eV) and Mn K-edge (6539 eV) for the ZnSe:xEu³⁺,yMn²⁺ (x and y = 12 mol%) core and ZnSe:Eu³⁺,Mn²⁺@ZnS (3 ML) core/shell QDs. XAFS data were measured with a double-crystal Si (111) monochromator and energy was calibrated according to the corresponding absorption K-edge of Zn and Mn metallic foils.

The samples were prepared in pallet form by pressing a homogeneous mixture of calculated quantity of finely ground material and polyvinylpyrrolidone (PVP) powder. The amount of material in each pellet was calculated using XAFS mass software to give an absorption $\mu_t \sim 1.5$, just above the Zn absorption K-edge. The X-ray absorption fine structure (XAFS) data of all the QDs were preprocessed in Athena from Demeter¹, including background subtraction, spectrum alignment and normalization. Whereas, the background R_{bkg} was set to 1.2 Å for the Fourier transforms of Eu L₃-edge and Zn K-edge EXAFS data of both the core and core/shell nanocrystals.

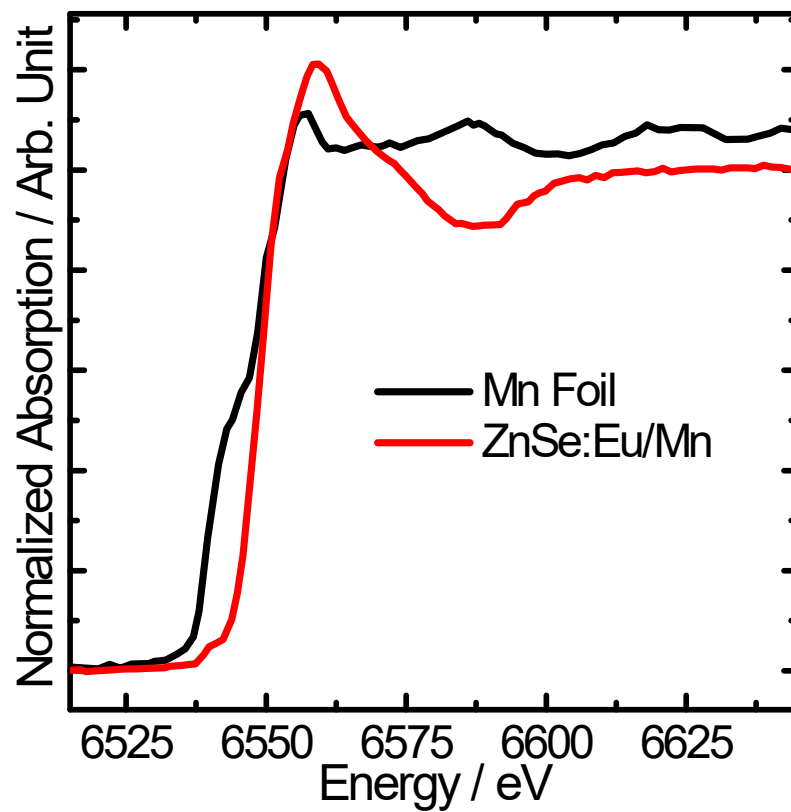


Figure S5. Normalized XANES spectra of the ZnSe:Eu³⁺,Mn²⁺@ZnS (3 ML) core/shell QDs and reference Mn foil collected at the Mn K-edge (6539 eV).

6. Photoluminescence spectra

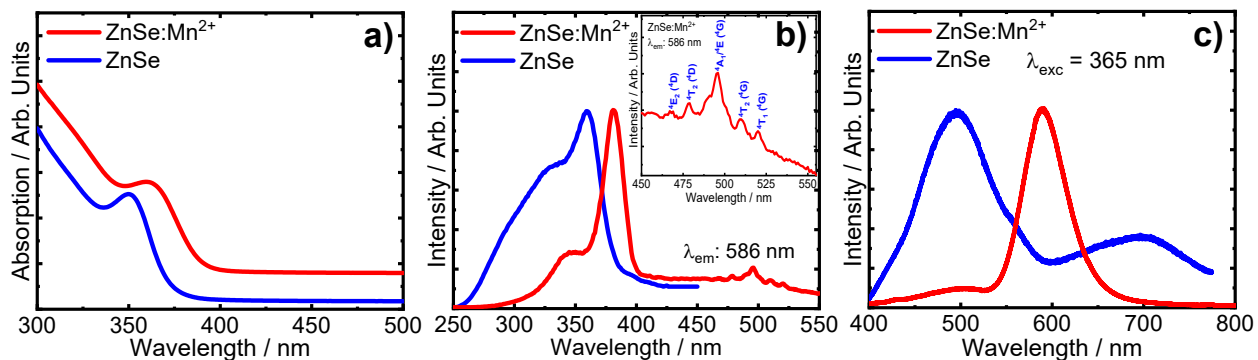


Figure S6. UV-visible absorption (a), excitation (b) and emission spectra (c) of ZnSe and ZnSe:Mn²⁺ (12 mol%) QDs. The inset figure b shows the excitation spectra of ZnSe:Mn²⁺ (12 mol%) QDs arising from the interconfigurational 3d⁵ transitions of Mn²⁺ ion.

7. CytoViva enhanced dark-field and dual-mode fluorescence (DMF) images of core QDs

The emission spectra of the ZnSe:Eu³⁺@ZnS (4 mol%) QDs showed red shift from 520 to 570 nm emission maximum under excitation at 445 and 520 nm, respectively. This behavior of QDs were also reflected by recording their CytoViva dual-mode fluorescence microscopy images, visualizing the green and red fluorescence images under irradiation at various wavelengths of 445 and 520 nm, respectively.

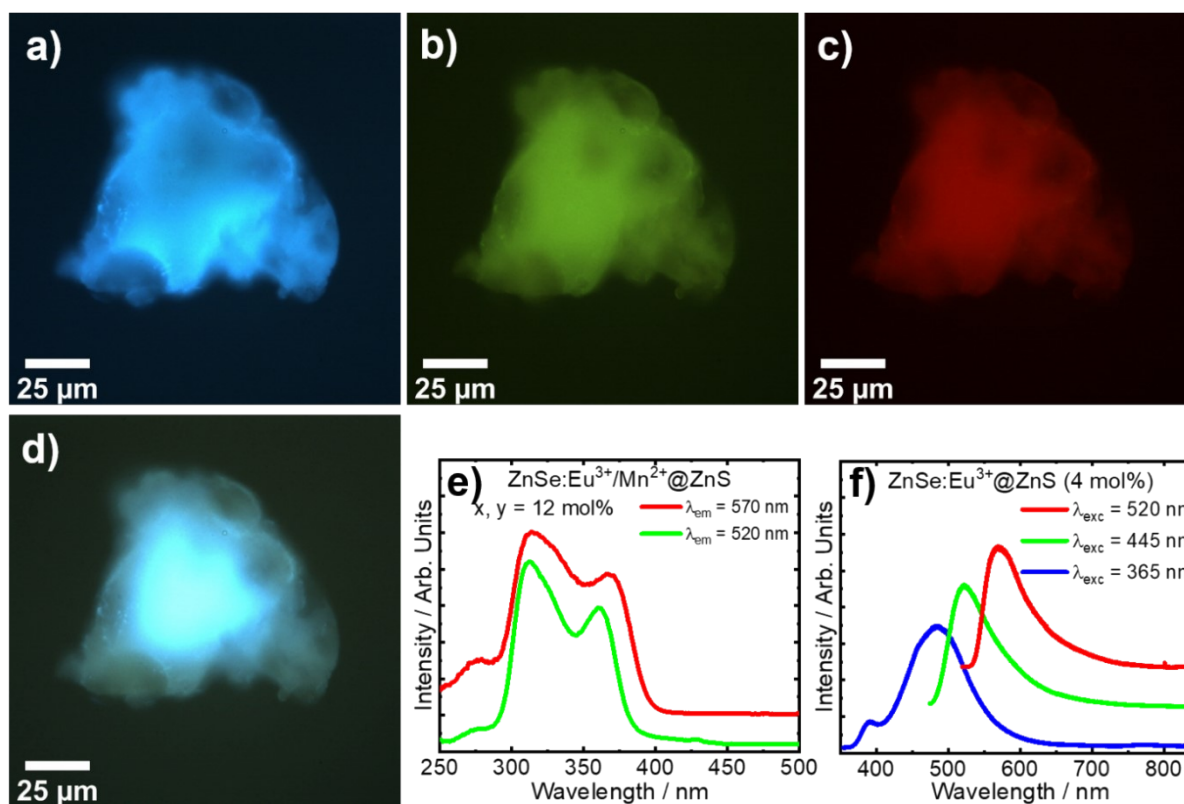


Figure S7. CytoViva dual-mode fluorescence images of ZnSe:Eu³⁺@ZnS (4 mol%) nanocrystals aggregates on the ultra-clean glass slide, measured at different excitation wavelengths (λ_{exc}): 390 nm (a), 445 nm (b), 520 nm (c), all the three wavelengths range (d) and the corresponding excitation (e) and emission (f) spectra.

8. CytoViva enhanced dark-field and dual-mode fluorescence images of core/shell QDs

The ZnSe:Eu³⁺,Mn²⁺@ZnS (x, y = 12 mol%) QDs, under excitation at 445 and 520 nm, exhibited broad emission spectra centered at 520 and 570 nm, respectively. The broadening of the emission bands towards lower energy when compared to that of ZnSe:Eu³⁺@ZnS (Figure S7) indicates the contribution by Mn²⁺, substantiating also the energy transfer from Eu³⁺ to Mn²⁺ ion. Similarly, the red shift in emission of these core/shell QDs under various excitation wavelengths was also demonstrated by recording their CytoViva dual-mode fluorescence microscopy images, which visualized the green and red fluorescence images under irradiation at various wavelengths of 445 and 520 nm, respectively. In addition, these core/shell QDs displayed pink fluorescence image under excitation at 390 nm, which is obvious from their emission spectrum, manifesting collective contribution of photo-generated electron-hole pair recombination emission of ZnSe (~497 nm) and Mn²⁺ ⁴T₁(⁴G)→⁶A₁(⁴S) emission (~586 nm) to their visualized pink color fluorescence.

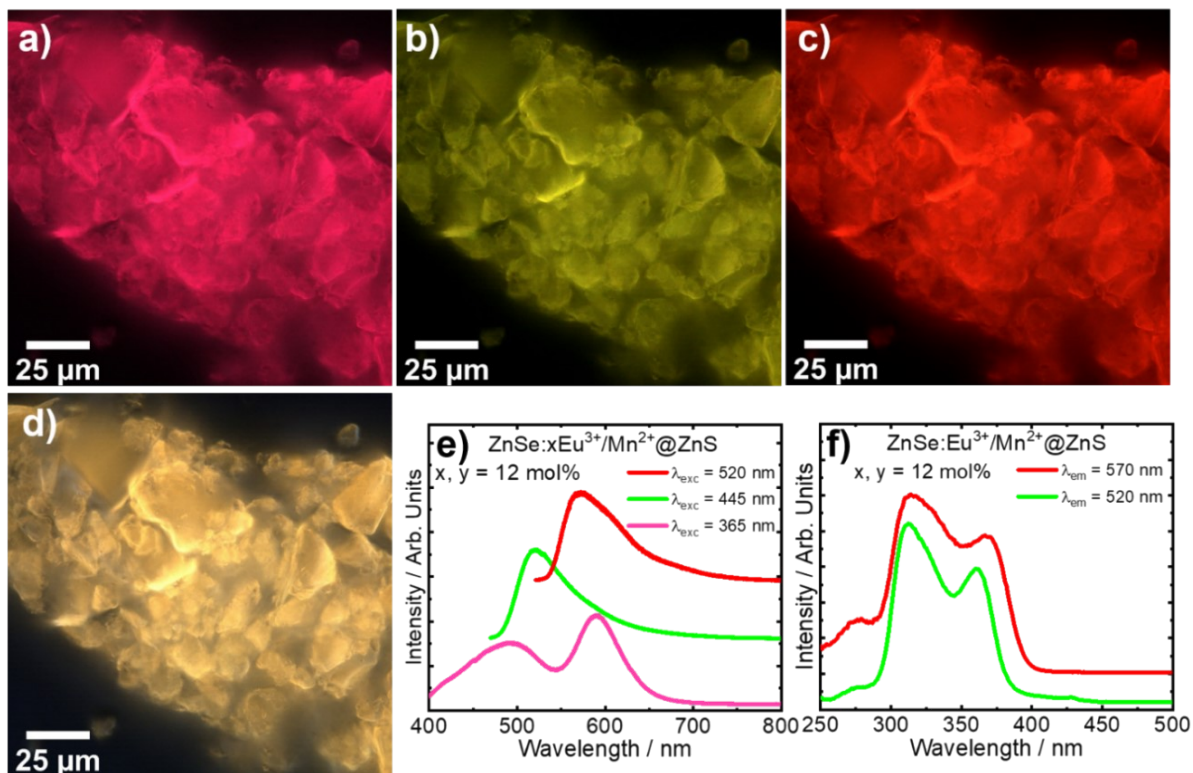


Figure S8. CytoViva dual-mode fluorescence images of aqueous ZnSe:xEu³⁺,yMn²⁺@ZnS (x, y = 12 mol%) core/shell QDs dispersion aggregates on ultra-clean glass slide, measured at different excitation wavelengths (λ_{exc}): 390 nm (a), 445 nm (b), 520 nm (c), all the three excitation wavelengths range (d), and the corresponding excitation (e) and emission (f) spectra.

9. Quantitative analyses of QDs uptake mechanism by FACS.

The cells were pretreated with different inhibitors, such as amiloride, PAO, MBCD, Cyt D, and 4 °C, over a period of 1 h and subsequently exposed to QDs for additional 3 h. After exposure to QDs, the medium was sucked up, and the cells were harvested by adding 200 µL/well of trypsin followed by incubating at 37 °C for 5 min. The enzymatic reaction was quenched by adding PBS fortified with FBS (10%), transferred each sample to an individual tube and subsequently centrifuged at 3000 rpm for 4 min. The cells were washed by PBS, resuspended in PBS (400 µl) and analyzed by flow cytometry FACS LSRFortessa (BD Biosciences), benefiting from the photoluminescence properties of QDs. The QDs were excited by three different lasers, i.e., violet ($\lambda = 405$ nm), blue ($\lambda = 488$ nm), and yellow-green ($\lambda = 561$ nm), and the change in fluorescence intensity was recorded at PE-Texas Red-A channel. The irregular changes in fluorescence intensity is linearly proportional to the amount of QDs internalized by cells or jointly with QDs probably attached to cell surfaces.

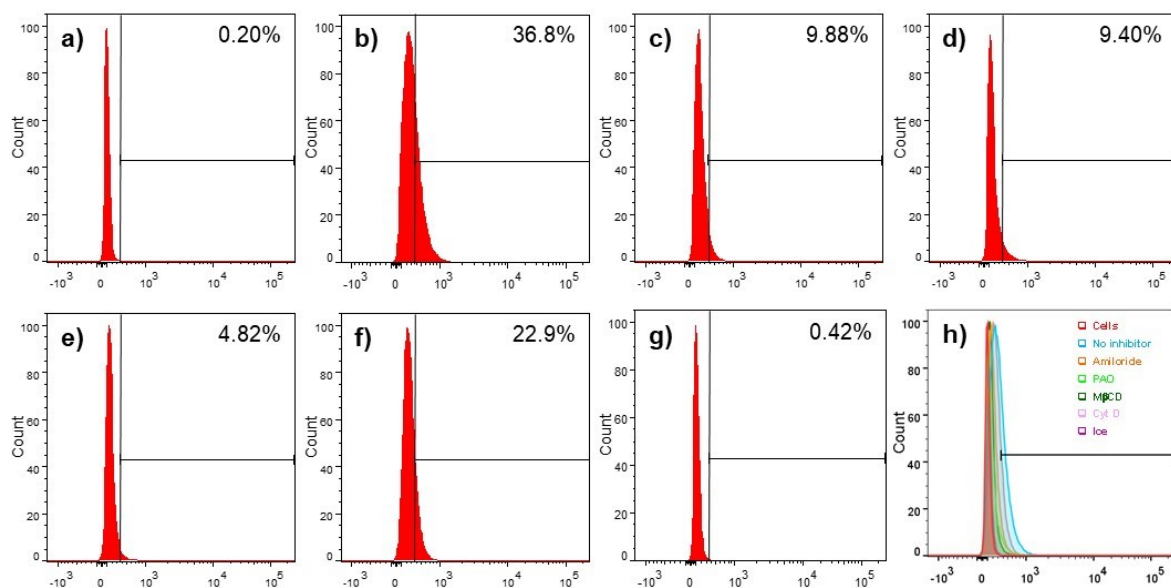


Figure S9. Flow cytometry analyses of cellular endocytosis of $\text{ZnSe}:x\text{Eu}^{3+},y\text{Mn}^{2+}@\text{ZnS}$ ($x, y = 12$ mol%) core/shell QDs treated with RAW cells at a concentration of $50 \mu\text{g mL}^{-1}$ for 3 h. The cells were rinsed several times with PBS and read by FACS under excitation at three different lasers, simultaneously: violet ($\lambda = 405$ nm), blue ($\lambda = 488$ nm) and yellow-green ($\lambda = 561$ nm). The change in fluorescence intensity was recorded at PE-Texas Red-A channels. The fluorescence intensity of treated samples was normalized to the auto-fluorescence of the negative control (untreated cells) (a), and the relative uptake (%) was calculated for positive control (QDs treated cells) (b), and cells treated with QDs in the presence of amiloride (c), PAO (d), $\text{M}\beta\text{CD}$ (e), Cyt D (f), 4°C (g), and joint histogram (h).

10. CytoViva enhanced dark-field and dual-mode fluorescence (DMF) images

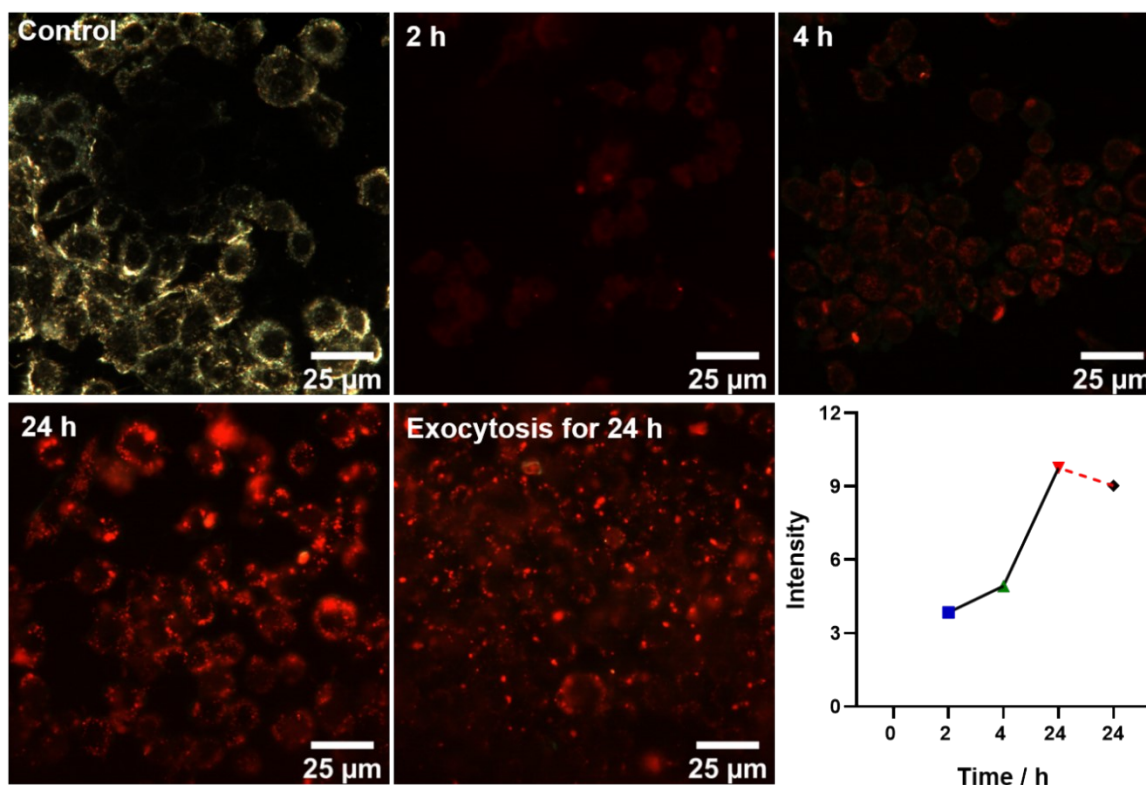


Figure S10. CytoViva enhanced dark-field and dual-mode fluorescence (DMF) images of time-dependent uptake and exocytosis in RAW macrophages treated with QDs ($100 \mu\text{g mL}^{-1}$) for 2, 4 and 24 h. For exocytosis, after exposure to QDs for 24 h, the medium was replaced by QDs-free fresh medium and incubated the cells for additional 24 h. The graph at the right bottom shows the change in fluorescence intensity as function of time. The red dotted line indicates the change in fluorescence intensity after exocytosis for 24 h.

References

- (1) Ravel, B.; Newville, M. ATHENA , ARTEMIS , HEPHAESTUS : Data Analysis for X-Ray Absorption Spectroscopy Using IFEFFIT. *J. Synchrotron Radiat.* **2005**, *12* (4), 537–541. <https://doi.org/10.1107/S0909049505012719>.